Effects of the hydration ratio on the electrosorption selectivity of ions during capacitive deionization

Yingzhen Li, Chang Zhang, Yanping Jiang, Ting-Jie Wang *, Haifeng Wang

Department of Chemical Engineering, Tsinghua University, Beijing 100084, China

HIGHLIGHTS

- Electrosorption selectivity in a competitive multi-ionic solution was studied.
- Monovalent ions with a low hydration ratio exhibit high selectivity.
- Divalent ions demonstrate higher selectivity than monovalent ions.
- The adsorbed ion is easily substituted by ions with lower hydration ratios.

GRAPHICAL ABSTRACT
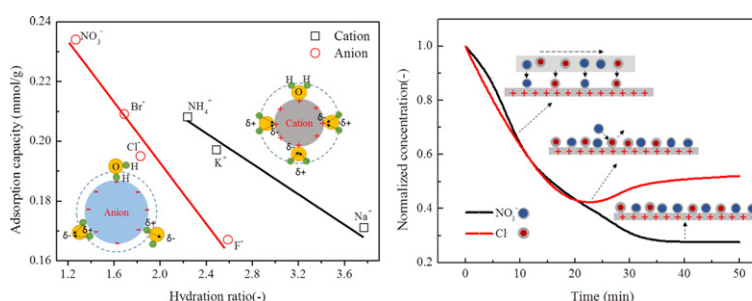
The hydration ratio, i.e., the ratio of hydrated radius to ion radius, significantly affects the electrosorption capacity and selectivity. Monovalent ions with a low hydration ratio exhibit high adsorption capacity and selectivity. The adsorbed ion is easily substituted by ions with lower hydration ratios or a higher valence.

ARTICLE INFO

ABSTRACT

The electrosorption performances of different ions in a capacitive deionization process were studied. The hydration ratio, i.e., the ratio of hydrated radius to ion radius, significantly affects the electrosorption capacity and selectivity. In a mono-ionic solution, ions with low hydration ratios exhibit high electrosorption capacities. The electrosorption capacity demonstrates a negative linear relationship with the hydration ratio for both anions and cations. In a multi-ionic solution, the monovalent ions with low hydration ratios exhibited high electrosorption selectivity. Divalent ions adsorb more easily onto electrode surface than monovalent ions do, resulting in higher electrosorption selectivity. In the late period of the electrosorption, the adsorbed ions were partly substituted by ions with lower hydration ratios or a higher valence. The hydration ratio and valence affect the ions' electrostatic attraction to the electrodes, determining the electrosorption capacity and selectivity of ions in capacitive deionization.

© 2016 Elsevier B.V. All rights reserved.

1. Introduction

Water shortage has become a worldwide problem due to water pollution and growing water demand. Desalination is an effective way to solve this problem [1,2]. Many methods are used to remove ions from water, including distillation, reverse osmosis, ion exchange, and electrodialysis. However, these processes often require high costs involving expensive investments, inconvenient operation, or high energy consumption [3–7]. Capacitive deionization (CDI) is an effective desalination process for water purification. Electrosorption has the advantages of high energy efficiency, high removal efficiency, low cost, and easy regeneration [8–11].

* Corresponding author.
  E-mail address: wangtj@tsinghua.edu.cn (T.-J. Wang).

An ideal electrode for CDI should possess a high specific surface area and high conductivity. Carbon materials with high specific surface area such as activated carbon (AC) [12–14], carbon fibers [15,16], carbon aerogels [17], carbon nanotubes [18], graphene [19,20], mesoporous carbon [21,22], and carbon composite materials [23,24] have been used to produce electrodes for electrosorption. Most recently, lots of novel electrode materials with various texture properties were rationally designed and developed for highly efficient capacitive deionization, such as the 3D hierarchical carbon [25], 3D graphene [26] and nitrogen-doped porous carbon [27]. Among these carbon materials, activated carbon is the most commonly used and economical material. Once an electric potential was applied on the carbon electrodes, the two electrodes become positively and negatively charged, respectively. When an aqueous solution flows through the gap between the two electrodes, anions move to the positive electrode, and cations move to the negative electrode due to electrostatic attraction, forming an electric double layer (EDL) on the electrode surface. The ions move to the electrode surface and are stored in the electric double layer, decreasing the salt concentration in the solution [28]. Once removing the electric potential, the adsorbed ions are released into the bulk solution, achieving electrode regeneration.

In an aqueous solution, large quantities of anions and cations are present. These ions compete with each other in the electrosorption process, leading to different electrosorption capacities and selectivities. For ions with different valences, Gabelich et al. [29] reported that monovalent ions with smaller hydrated radii were more effectively removed from a solution than multivalent ions with larger hydrated radii. However, some contrary conclusions have also been reported. Hou et al. [30] reported that divalent cations were more effectively removed than monovalent cations, and Zhao et al. [31] also reported that selectivity of Ca^{2+} over Na^+. For monovalent ions, Hou et al. [30] reported that ions with smaller hydrated radii exhibited higher selectivity due to size-affinity, e.g., K^+ (the hydrated radius is 3.31 Å) had higher selectivity than Na^+ (the hydrated radius is 3.58 Å). Pei et al. [32] and Dykstra et al. [33] also reported the same results. For divalent ions, ions with a smaller hydrated radius were also more easily removed, e.g., Ca^{2+} (the hydrated radius is 4.12 Å) exhibited higher selectivity than Mg^{2+} (the hydrated radius is 4.28 Å) [32,34].

The size-affinity explanation [30] indicates that the ions with smaller hydrated radii demonstrate higher selectivity. Han et al. [35] reported that the electrosorption capacity had a roughly linear relationship with the hydrated radius size, but when the hydrated radii of different ions were similar in size, this relationship involved large errors. In some cases, the ion with the smaller hydrated radius exhibited lower electrosorption capacity. In the work by Gabelich et al. [29], NO_3^- possessed higher selectivity than Cl^-, even though NO_3^- has a larger hydrated radius. Chen et al. [36] reported that the adsorbed Cl^- could be substituted by NO_3^- in the electrosorption process, which also implies that NO_3^- with its larger hydrated radius demonstrated higher electrosorption selectivity than Cl^- did. In fact, the hydrated radii difference between these ions is very tiny. For example, the hydrated radii difference of NO_3^- and Cl^- is only 0.03 Å; however, their electrosorption selectivities differed greatly [36]. Even for ions with the same hydrated radii, e.g., K^+ and NH_4^+ in this work, their electrosorption capacities and selectivities can differ significantly. The size-affinity explanation cannot explain why the ion with larger hydrated radii had higher electrosorption selectivity. The key factors affecting the electrosorption selectivity of ions remains unclear.

In this paper, a dimensionless parameter of hydration ratio, i.e., the ratio of hydrated radius to ion radius, was found to be the key factor affecting ion electrosorption selectivity. Activated carbon with a high specific area was used to produce the electrodes. The electrosorption capacity and ion selectivity in mono-ionic and multi-ionic solutions were experimentally studied, respectively.

2. Materials and methods

2.1. Fabrication of AC electrodes

AC with a specific surface area of 2130 m²/g (Fuzhou Yi-Huan Carbon, China) was used to prepare the electrodes. To fabricate the carbon electrodes, a carbon slurry was prepared by mixing AC powder, carbon black (Fuzhou Yi-Huan Carbon, China), and a solution of poly(vinylidene fluoride) (PVDF, MW = 275,000, Sigma-Aldrich, USA) dissolved in dimethylacetamide (DMAc, Beijing Chemical Reagents, China). The slurry was stirred for 3 h to obtain a homogeneous mixture and then coated on a graphite plate. The AC, carbon black conductive material, and PVDF binder were present in the slurry at a fraction ratio of 8:1:1. The coated plate was dried in an oven at 80 °C for 6 h and then placed in a vacuum oven at 50 °C for 2 h to completely remove any organic solvent remaining in the micropores of the coated layer. The AC electrodes were then assembled into an electrosorption cell.

2.2. Electrosorption apparatus and experiments

The schematic diagram of the electrosorption apparatus used is shown in Fig. 1. A hole with a diameter of 6 mm was opened for water to flow through. Before each experiment, the electrosorption cell was washed with deionized water to remove any salts remaining in the experimental system. During the electrosorption process, the salt solution was fed through a peristaltic pump into the electrosorption cell, and then the effluent was returned to the feed tank. The solution was circulated until electrosorption equilibrium was reached. The equilibrium concentration of different ions was measured by ion chromatography. The equilibrium electrosorption capacity was defined as

$$Q(\text{mmol/g}) = \frac{(C_0 - C_e)V}{m}$$

where Q is the equilibrium electrosorption capacity, mmol/g (AC); C_0 and C_e are the initial and equilibrium concentrations of ion, respectively, mmol/L; V is the volume of the circulated solution, L, i.e., 50 mL in this work; and m is the AC mass on the electrode, g.

To investigate the electrosorption selectivity of different ions, a multi-ionic solution was prepared by mixing solutions of different ions. To compare their selectivity, the initial concentration of each ion was set as equal, and the total ion concentration of the solution was maintained at approximately 2 mmol/L. F^-, Cl^-, Br^-, and NO_3^- were selected as the monovalent anions, and Na^+ was used to balance the anions. Na^+, K^+, and NH_4^+ were selected as the monovalent cations, and Cl^- was used to balance the cations.
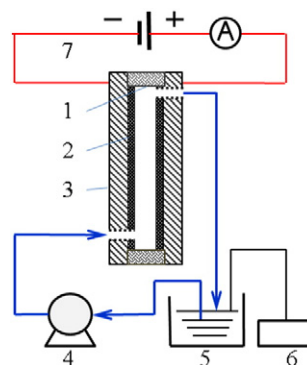

Fig. 1. Schematic of the experimental apparatus for electrosorption. 1. Insulated spacer; 2. AC electrode; 3. graphite plate; 4. peristaltic pump; 5. feed tank; 6. ion chromatograph; 7. potentiostat.

2.3. Hydration ratio

Ions in aqueous solutions carry an ionic charge, which forms an electric field around the ions. Ions with a smaller radius and higher valence possess higher surface charge density, which forms a stronger electric field to polarize the water molecules on the ions' surface [37, 38]. Usually, the stronger the electric polarization is, the more water molecules are fixed on the surface, and the larger is the hydrated radius of the ion. Therefore, ions with smaller radii have larger hydrated radii. For example, the hydrated radius of F^- is higher than that of other monovalent anions, and the divalent Ca^{2+} has a larger hydrated radius than does monovalent K^+. The radii of cations are usually smaller than those of anions, so cations typically have more hydrated water molecules on their surface.

Fig. 2 shows that water molecules are polarized on the ion surface. The polarized water molecules form a hydration layer on the ion surface. For cations, the negatively charged oxygen of the water molecule contacts the positive ionic charge. For anions, the positively charged hydrogen of the water molecule contacts the negative ionic charge. Therefore, the ionic charges of ions are partly screened by the polarized water molecules.

To describe the electric polarization strength, a dimensionless parameter of hydration ratio was defined, i.e., the ratio of hydrated radius to ion radius. A larger hydration ratio reflects stronger electric polarization and stronger electric screening acting on the ionic charge. The ion radius, hydrated radius, and hydration ratio of the different ions used in this work are listed in Table 1.

3. Results and discussion

3.1. Electrosorption capacity of monovalent anions

The electrosorption capacities of monovalent anions F^-, Cl^-, Br^-, and NO_3^- were measured. The initial anion concentration of each solution was 2 mmol/L. During the electrosorption process, a voltage of 1.2 V was applied until electrosorption equilibrium was reached, and then the electrodes were shorted for regeneration. The normalized concentration was used to evaluate the removal efficiency of anions, which is shown in Fig. 3. Once removing the applied voltage, all of the adsorbed ions were released back into the bulk solution, indicating that no specific adsorption occurred in the electrosorption process, and all of the adsorption capacity was contributed by the electrosorption. At the electrosorption time of 40 min, which was close to the electrosorption equilibrium, the removal efficiencies for anions were in the order of $NO_3^- > Br^- > Cl^- > F^-$. The electrosorption capacity of anions is listed in Table 2.

From the size-affinity explanation, the ions with smaller hydrated radii were deduced to possess higher electrosorption capacities. As seen in Table 1, the hydrated radii of the four anions are in the order of F^- (3.52 Å) > NO_3^- (3.35 Å) > Cl^- (3.32 Å) > Br^- (3.30 Å). F^- has the largest hydrated radius (3.52 Å), which is obvious higher than those of other anions, and it had the lowest capacity of 0.167 mmol/g, which fit the size-affinity explanation. However, the hydrated radii of
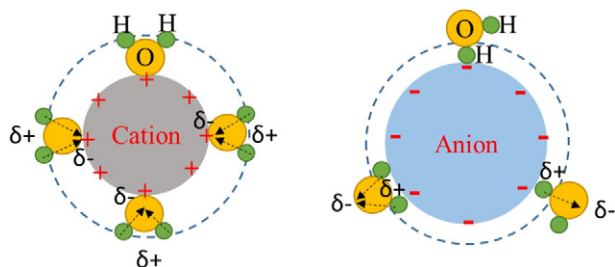
Table 1
The radius, hydrated radius, and hydration ratio of different ions used in this work. [37].

Ion	F^-	Cl^-	Br^-	NO_3^-	SO_4^{2-}	Na^+	K^+	NH_4^+	Ca^{2+}
Ion radius, Å	1.36	1.81	1.95	2.64	2.90	0.95	1.33	1.48	0.99
Hydrated radius, Å	3.52	3.32	3.30	3.35	3.79	3.58	3.31	3.31	4.12
Hydration ratio, —	2.59	1.83	1.69	1.27	1.31	3.77	2.49	2.24	4.16

NO_3^- (3.35 Å), Cl^- (3.32 Å), and Br^- (3.30 Å) were very similar, and NO_3^- exhibited the greatest electrosorption capacity, 0.234 mmol/g, which was higher than those of Cl^- and Br^-. The size-affinity explanation does not fit the result that the ion with a larger hydrated radius had a higher electrosorption capacity. However, we observed that the hydration ratio of the four monovalent anions followed the order of NO_3^- (1.27) < Br^- (1.69) < Cl^- (1.83) < F^- (2.59), which displayed an inverse relationship with electrosorption capacity, implying that the anion with smaller hydration ratio possess higher electrosorption capacity.

In the CDI process, ions are adsorbed onto the electrode surface by electrostatic attraction. Because the water molecules on the ion surface are polarized, the polarized hydrated water layer causes some electrostatic screening on the ionic charge, as shown in Fig. 2. The ionic charge was partly screened by the polarized water molecules, weakening the electrostatic attraction that acted on the ions. The stronger the polarization was, the stronger the electrostatic screening was. A higher hydration ratio indicates stronger electrostatic screening, leading to a weaker electrostatic attraction that acted on the ions. Because F^- has the highest hydration ratio, so it had the weakest electrostatic attraction, leading to the lowest electrosorption capacity. NO_3^- with the lowest hydration ratio had the highest electrosorption capacity. The electrosorption capacities under different initial anion concentration were also studied, and the results are shown in Fig. 4. Under the initial concentration of 1 mmol/L, 2 mmol/L and 10 mmol/L, the electrosorption capacity of the monovalent anions demonstrated a negative linear relationship with the hydration ratio, as shown in Fig. 4. It shows that the hydration ratio is the key factor to determine the electrosorption capacity of monovalent anions under varied initial concentration. Ions with lower hydration ratios are inferred to possess higher electrosorption capacities.

3.2. Electrosorption selectivity of anions

The electrosorption selectivity of anions was investigated in dual anion solutions. Mixed solutions of F-Cl, F-Br, F-NO_3, Cl-Br, Cl-NO_3, and

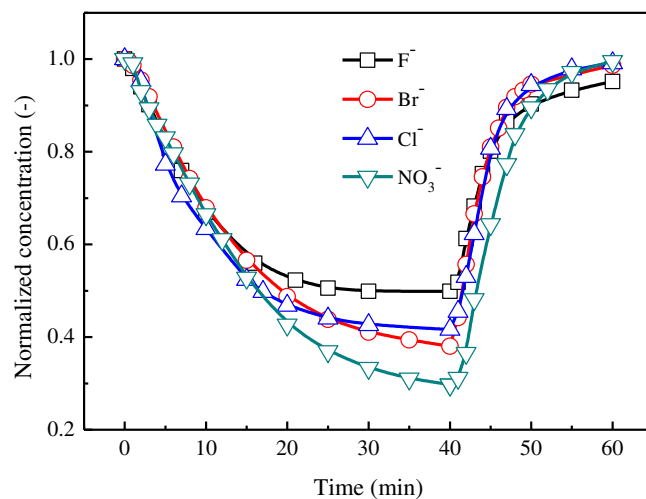**Fig. 2.** Polarized water molecules on the ion surface.

Fig. 3. The electrosorption performance for different monovalent anions under an applied voltage of 1.2 V (initial anion concentration: 2 mmol/L).

Table 2
Electrosorption capacity of different monovalent anions under applied voltage 1.2 V (Initial anion concentration: 2 mmol/L, electrosorption time: 40 min).

Anion	F^-	Cl^-	Br^-	NO_3^-
Capacity, mmol/g	0.167	0.195	0.207	0.234

Br-NO$_3$ were prepared. The initial concentration of each anion was set at 1 mmol/L to keep the total ion concentration at approximately 2 mmol/L. Electrosorption under an applied voltage of 1.2 V was conducted for 90 min to ensure that the solution reached equilibrium. The anion concentration in each dual anion solution was measured, and the removal efficiency of the anion was calculated, with the results listed in Table 3.

By comparing their removal efficiency in the dual anion solution, the electrosorption selectivity of the anions was determined. For example, in the Cl-NO$_3$ solution, NO$_3^-$ had a removal efficiency of 72%, and Cl$^-$ had 50%, indicating that NO$_3^-$ exhibited higher electrosorption selectivity than Cl$^-$. In the F-Cl solution, Cl$^-$ had a removal efficiency of 71%, higher than that of F$^-$ (i.e., Cl$^-$ had higher electrosorption selectivity). The electrosorption selectivity for anions in six kinds of dual anion solution is in the order of $F^- < Cl^-$, $F^- < Br^-$, $F^- < NO_3^-$, $Cl^- < Br^-$, $Cl^- < NO_3^-$ and $Br^- < NO_3^-$, respectively. From this results, the electrosorption selectivity of the anions are listed in the order of $NO_3^- > Br^- > Cl^- > F^-$.

To further verify the selectivity order of the ions in a competitive multi-ionic solution, the electrosorption selectivity of monovalent anion was also investigated in a four anion solution, i.e., a mixed solution of NaF, NaCl, NaBr, and NaNO$_3$. The initial concentration of each anion was set at 0.5 mmol/L in the mixed solution. The removal efficiency of each monovalent anion was measured and the result is listed in Table 4. The removal efficiency of the four monovalent anions followed the order of NO_3^- (80%) > Br^- (72%) > Cl^- (20%) > F^- (4%), confirming that the electrosorption selectivity of the monovalent anions is in the order of $NO_3^- > Br^- > Cl^- > F^-$. This result is consistent with the conclusion obtained from the dual anion solution studies. The removal efficiency of the NO$_3^-$ was 20-fold higher than that of F$^-$, indicating that their selectivity differed greatly in the multi-ionic solution. The competitive effect of the different ions is significant. The AC used in this work is a micropore-dominant material with a surface area of 2130 m^2/g and average pore size of 1.3 nm [39]. This pore size results in high diffusion resistance for ions. The ion with lower hydration ratio possesses higher electrostatic attraction that is easier to overcome the diffusion resistance and be adsorbed on the electrode surface, which enlarge the difference of the electrosorption selectivity.
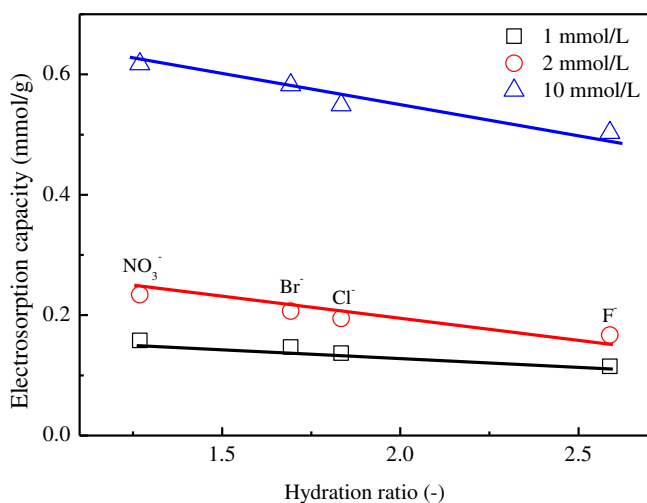

Fig. 4. The linear fitting of the electrosorption capacity of monovalent anions vs. their hydration ratio under different initial concentration.

Table 3
The selectivity of anions in a dual anion solution. (Initial concentration of each anion: 1 mmol/L, applied voltage: 1.2 V, electrosorption time: 90 min).

Dual anion solution	F-Cl		F-Br		F-NO$_3$		Cl-Br		Cl-NO$_3$		Br-NO$_3$	
Anion	F^-	Cl^-	F^-	Br^-	F^-	NO_3^-	Cl^-	Br^-	Cl^-	NO_3^-	Br^-	NO_3^-
Removal efficiency, %	31	71	28	70	22	80	35	78	50	72	33	81

According to the size-affinity explanation, ions with smaller hydrated radii had higher selectivities. F$^-$ has the largest hydrated radius, and it demonstrated the lowest electrosorption selectivity. However, NO$_3^-$ (3.35 Å), Br$^-$ (3.30 Å), and Cl$^-$ (3.32 Å) possess little difference in their hydrated radii, with Br$^-$ having the smallest hydrated radius, but Br$^-$ did not exhibit the highest electrosorption selectivity.

For ions with same valence, the ion with the lowest hydration ratio demonstrates the strongest electrostatic attraction. Therefore, the ions with lower hydration ratio more easily adsorb onto the electrode surface and have higher electrosorption selectivity. The electrosorption selectivity of the monovalent anions follows the order of $NO_3^- > Br^- > Cl^- > F^-$.

3.3. Ion competition in electrosorption process

To further investigate the competition of the different anions in the electrosorption process, a mixed solution of NO$_3^-$ and Cl$^-$ with the same initial concentrations was prepared. During the electrosorption process, the concentrations of NO$_3^-$ and Cl$^-$ were measured, and the results are shown in Fig. 5. During the early part of the electrosorption process, NO$_3^-$ and Cl$^-$ exhibited almost the same electrosorption rate. Because NO$_3^-$ and Cl$^-$ possess the same valence and similar hydrated radii, they diffused into the EDL on the electrode surface, and no competition occurred between NO$_3^-$ and Cl$^-$ during the early period. However, as NO$_3^-$ and Cl$^-$ were continuously adsorbed on the electrode surface, the EDL was gradually filled until reaching equilibrium. Due to the limitations of the EDL capacity, the competitive effect between NO$_3^-$ and Cl$^-$ became obvious in the later period of the electrosorption process. Fig. 5 shows that the NO$_3^-$ and Cl$^-$ concentration difference became obvious when the electrosorption time exceeded 20 min. The concentration of NO$_3^-$ decreased continuously, while the concentration of Cl$^-$ began to increase. This result suggests that some adsorbed Cl$^-$ was repelled out of the EDL and substituted by NO$_3^-$. After 50 min, the electrosorption reached equilibrium, and almost 10% of the adsorbed Cl$^-$ was substituted by NO$_3^-$, indicating that the electrosorption selectivity of NO$_3^-$ was higher than that of Cl$^-$. This difference is because NO$_3^-$ has lower hydration ratio and weaker electrostatic screening, so the electrostatic attraction acting on NO$_3^-$ is stronger, leading to Cl$^-$ substitution by NO$_3^-$. Chen et al. [36] also reported that the adsorbed Cl$^-$ was partly substituted by NO$_3^-$ in using activated carbon as electrodes. The substitution is well explained by the hydration ratio proposed in this work.

The electrosorption competition of ions with different valences was also investigated. A mixed solution with the same initial concentration of SO$_4^{2-}$ and NO$_3^-$ (1 mmol/L) was prepared. The changes in the concentrations of SO$_4^{2-}$ and NO$_3^-$ with the electrosorption time are shown in Fig. 6. The divalent SO$_4^{2-}$ exhibited a higher electrosorption rate than the monovalent NO$_3^-$ did during the early period of the electrosorption process. Some adsorbed NO$_3^-$ was substituted by SO$_4^{2-}$ in the late period

Table 4
The electrosorption selectivity of monovalent anions in a four anion solution. (Initial concentration: 0.5 mmol/L, applied voltage: 1.2 V, electrosorption time: 90 min).

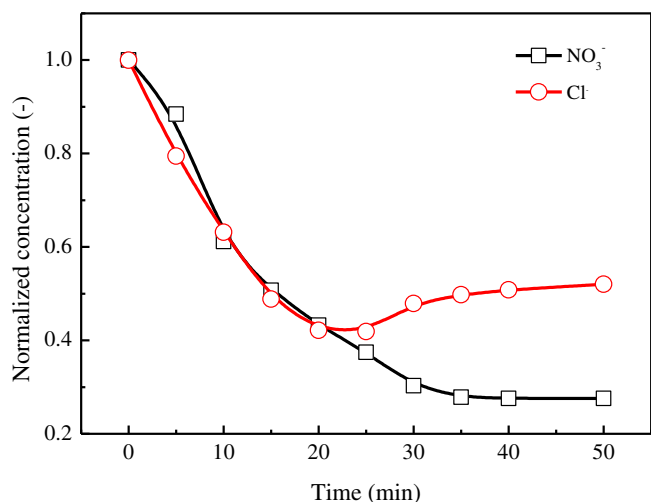| Anion	F^-	Cl^-	Br^-	NO_3^-
Removal efficiency, %	4	20	72	80

Fig. 5. The electrosorption competition of NO_3^- and Cl^- under an applied voltage of 1.2 V (the initial concentration of each anion was 1 mmol/L).
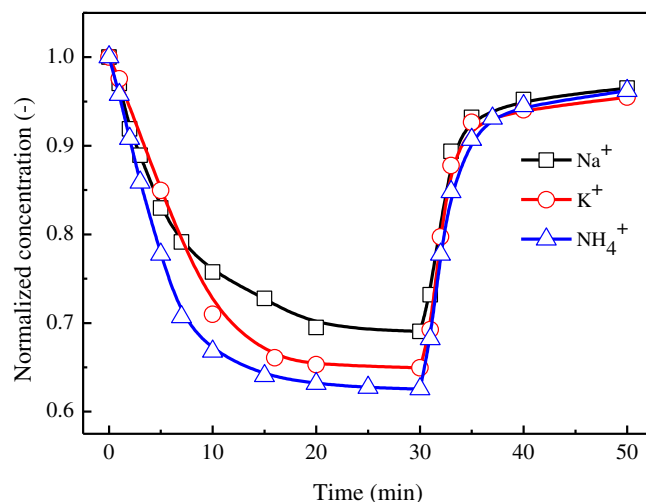

Fig. 7. The electrosorption performance of Na^+, K^+, and NH_4^+ under an applied voltage of 1.2 V (the initial concentration of each cation was 2 mmol/L).

of the electrosorption due to the SO_4^{2-} ion's stronger electrostatic attraction. The electrosorption process reached equilibrium after 60 min. The removal efficiency of SO_4^{2-} was 39%, higher than the removal efficiency of 19% for NO_3^-. This result indicates that the electrosorption selectivity of the divalent SO_4^{2-} is higher than that of the monovalent NO_3^-.

For the ions with different valences, the electrostatic attraction is mainly determined by the valence, rather than the hydration ratio. Although divalent ions exhibit stronger electrostatic screening caused by their higher hydration ratio, their effective ionic charge is still obvious higher than monovalent ions due to the higher valence. Therefore, divalent ions are more easily adsorbed on the electrode surface. Because the electrostatic attraction acting on the divalent SO_4^{2-} was stronger, part of the adsorbed NO_3^- was substituted by SO_4^{2-}, indicating that SO_4^{2-} has higher electrosorption selectivity than NO_3^-.

3.4. Electrosorption capacity and selectivity of the cations

The electrosorption capacities of the monovalent cations Na^+, K^+, and NH_4^+ were investigated. NaCl, KCl, and NH_4Cl solutions were used in the electrosorption process at the same initial concentration. Electrosorption was conducted under an applied voltage of 1.2 V, until reaching equilibrium. The desorption was conducted by shorting the

electrodes. The electrosorption and desorption performances of Na^+, K^+, and NH_4^+ are shown in Fig. 7. NH_4^+ was found to exhibit the highest capacity, and Na^+ had the lowest one. Once the applied voltage was removed, all of the adsorbed NH_4^+, K^+, and Na^+ were released back into the bulk solution, indicating that no specific adsorption occurred in the electrosorption process.

The change in electrosorption capacity with the hydration ratio is shown in Fig. 8. The electrosorption capacity of the monovalent cations demonstrated a negative linear relationship with the hydration ratio. The hydration ratio of the three monovalent cations followed the order of Na^+ (3.77) > K^+ (2.49) > NH_4^+ (2.24), and their electrosorption capacities were in the reverse order of $Na^+ < K^+ < NH_4^+$, indicating that the cations with lower hydration ratio exhibit higher electrosorption capacity.

The electrosorption selectivity of Na^+ and K^+ in a dual cation solution of NaCl and KCl was investigated. The removal efficiency of Na^+ and K^+ was 43.9% and 53.3%, respectively, indicating that K^+ has higher selectivity. The electrosorption selectivity of monovalent Na^+, K^+, and NH_4^+ was further investigated using a mixed solution of NaCl, KCl, and NH_4Cl. The initial concentration of each cation was set at 0.7 mmol/L to keep the total ion concentration at approximately 2 mmol/L. After reaching the electrosorption equilibrium, the removal efficiency of Na^+, K^+, and NH_4^+ were measured to be 34.7%, 52.1%, and 62%,
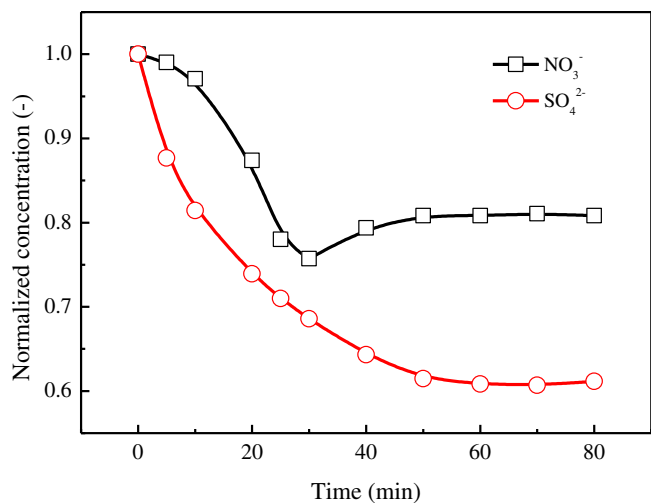

Fig. 6. The electrosorption competition of SO_4^{2-} and NO_3^- under an applied voltage of 1.2 V (the initial concentration of each anion was 1 mmol/L).
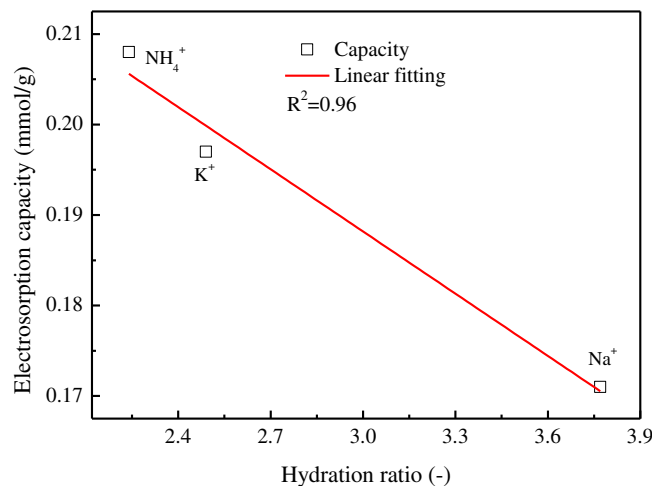

Fig. 8. The linear fitting of electrosorption capacity vs. the hydration ratio (initial concentration: 2 mmol/L, applied voltage: 1.2 V, electrosorption time: 30 min).

respectively. The hydrated radii of the three cations follows the order of Na$^+$ (3.58 Å) > K$^+$ (3.31 Å) = NH$_4^+$ (3.31 Å). Na$^+$ with the highest hydrated radius exhibited the lowest removal efficiency of 34.7%, i.e., the lowest electrosorption selectivity. Although K$^+$ and NH$_4^+$ had the same hydrated radii, the removal efficiency of K$^+$ (52.1%) was lower than that of NH$_4^+$ (62%), i.e., the electrosorption selectivity of K$^+$ was lower than that of NH$_4^+$. The size-affinity explanation cannot explain the result that the ions with the same hydrated radii size demonstrated different electrosorption selectivities. However, these results can be well explained using the hydration ratio. The hydration ratio of the three monovalent cations follows the order of Na$^+$ (3.77) > K$^+$ (2.49) > NH$_4^+$ (2.24), and their electrosorption selectivity are in the reverse order of Na$^+$ < K$^+$ < NH$_4^+$. The electrosorption selectivity of the monovalent cations also confirms that the ion with lower hydration ratio exhibits higher electrosorption selectivity.

The electrosorption selectivity of the cations with different valences was investigated using a mixed solution of monovalent K$^+$ and divalent Ca^{2+}. The initial concentrations of K$^+$ and Ca^{2+} were both set at 1 mmol/L. After the electrosorption reached equilibrium, the concentrations of K$^+$ and Ca^{2+} were measured, and the removal efficiency was calculated to be 15% and 55%, respectively. The removal efficiency of Ca^{2+} was obviously higher than that of K$^+$, indicating that Ca^{2+} has higher electrosorption selectivity. Ca^{2+} possesses a hydration ratio of 4.16, higher than that of K$^+$, indicating the stronger electric screening that acts on Ca^{2+}. However, although Ca^{2+} has stronger electric screening caused by polarized water molecules, its effective ionic charge is higher than that of the monovalent K$^+$, so the electrostatic attraction that acts on Ca^{2+} is higher than that on K$^+$, leading to the higher electrosorption selectivity. In this work, the electrosorption selectivity of cations are in the order of Ca^{2+} > K$^+$ > Na$^+$. The same results were also obtained in the electrosorption process using other carbon-based electrodes, such as activated carbon electrodes [30], carbon aerogel electrodes [32] and activated carbon cloth electrodes [40]. All of these results are well explained by using the hydration ratio and valence.

For monovalent anions and cations, the hydration ratio determines the electrosorption selectivity. The ion with lower hydration ratio demonstrates higher electrosorption selectivity due to the stronger electrostatic attraction acting on that ion. For ions with different valences, the valence determines their electrosorption selectivity. Divalent ions have higher effective ionic charges due to their higher valence than monovalent ions, so divalent ions are more easily adsorbed onto the electrode surface, leading to higher electrosorption selectivity.

4. Conclusions

The electrosorption performance of ions in a competitive multi-ionic solution was studied using activated carbon electrode. The hydration ratio, i.e., the ratio of the hydrated radius to ion radius, which reflects the electric polarization strength of the hydrated layer, was found to determine the electrostatic attraction that acts on the various ions, resulting in different electrosorption capacities and selectivities.

In the mono-ionic solution, the ion with lower hydration ratio exhibits higher electrosorption capacity, and the electrosorption capacity demonstrates a negative linear relationship with the hydration ratio for both monovalent anions and monovalent cations at the same initial concentration. In the multi-ionic solution, the ion with lower hydration ratio has higher electrosorption selectivity. The selectivity of the monovalent cations follows the order Na$^+$ < K$^+$ < NH$_4^+$, and that of anions were in the order NO$_3^-$ > Br$^-$ > Cl$^-$ > F$^-$.

In the Cl$^-$ and NO$_3^-$ solution, the adsorbed Cl$^-$ was partly substituted by NO$_3^-$ with a lower hydration ratio during the later period of the electrosorption process. In the NO$_3^-$ and SO$_4^{2-}$ solution, the adsorbed NO$_3^-$ was partly substituted by SO$_4^{2-}$ with a higher valence in the later period of the electrosorption process. Divalent ions exhibit higher selectivity than monovalent ions do.

References

[1] H. Yin, S. Zhao, J. Wan, H. Tang, L. Chang, L. He, H. Zhao, Y. Gao, Z. Tang, Three-dimensional graphene/metal oxide nanoparticle hybrids for high-performance capacitive deionization of saline water, Adv. Mater. 25 (2013) 6270–6276.
[2] T.P. Barnett, J.C. Adam, D.P. Lettenmaier, Potential impacts of a warming climate on water availability in snow-dominated regions, Nature 438 (2005) 303–309.
[3] B. Jia, L. Zou, Graphene nanosheets reduced by a multi-step process as high-performance electrode material for capacitive deionization, Carbon 50 (2012) 2315–2321.
[4] Z. Wang, L. Yue, Z.T. Liu, Z.H. Liu, Z. Hao, Functional graphene nanocomposite as an electrode for the capacitive removal of FeCl$_3$ from water, J. Mater. Chem. 22 (2012) 14101–14107.
[5] Z. Peng, D. Zhang, L. Shi, T. Yan, S. Yuan, H. Li, R. Gao, J. Fan, Comparative electroadsorption study of mesoporous carbon electrodes with various pore structures, J. Phys. Chem. C 115 (2011) 17068–17076.
[6] Y.A.C. Jande, W.S. Kim, Predicting the lowest effluent concentration in capacitive deionization, Sep. Sci. Technol. 115 (2013) 224–230.
[7] X. Wen, D. Zhang, L. Shi, T. Yan, H. Wang, J. Zhang, Three-dimensional hierarchical porous carbon with a bimodal pore arrangement for capacitive deionization, J. Mater. Chem. 22 (2012) 23835–23844.
[8] C.Y. Ma, S.C. Huang, P.H. Chou, C.Y. Maa, W. Denb, C.H. Hou, Application of a multiwalled carbon nanotube-chitosan composite as an electrode in the electrosorption process for water purification, Chemosphere 146 (2016) 113–120.
[9] K. Shi, L. Zhitomirsky, Supercapacitor devices for energy storage and capacitive dye removal from aqueous solutions, RSC Adv. 5 (2015) 320–327.
[10] B.H. Park, J.H. Choi, Improvement in the capacitance of a carbon electrode prepared using water-soluble polymer binder for a capacitive deionization application, Electrochim. Acta 55 (2010) 2888–2893.
[11] L. Chao, Z. Liu, G. Zhang, X.N. Song, X.D. Lei, M. Noyong, U. Simon, Z. Chang, X.M. Sun, Enhancement of capacitive deionization capacity of hierarchical porous carbon, J. Mater. Chem. A 3 (2015) 12730–12737.
[12] C.L. Yeh, H.C. Hsi, K.C. Li, C.H. Hou, Improved performance in capacitive deionization of activated carbon electrodes with a tunable mesopore and micropore ratio, Desalination 367 (2015) 60–68.
[13] K.H. Park, D.H. Kwak, Electrosorption and electrochemical properties of activated-carbon sheet electrode for capacitive deionization, J. Electroanal. Chem. 732 (2014) 66–73.
[14] J.H. Choi, Fabrication of a carbon electrode using activated carbon powder and application to the capacitive deionization process, Sep. Purif. Technol. 70 (2010) 362–366.
[15] G. Wang, C. Pan, L. Wang, Q. Dong, C. Yu, Z.B. Zhao, J.S. Qiu, Activated carbon nanofiber webs made by electrospinning for capacitive deionization, Electrochim. Acta 69 (2012) 65–70.
[16] Y. Chen, M. Yue, Z.H. Huang, F. Kang, Electrospun carbon nanofiber networks from phenolic resin for capacitive deionization, Chem. Eng. J. 252 (2014) 30–37.
[17] K.L. Yang, S. Yiacoumi, C. Tsouris, Electrosorption capacitance of nanostructured carbon aerogel obtained by cyclic voltammetry, J. Electroanal. Chem. 540 (2003) 159–167.
[18] M.A. Tofighy, T. Mohammadi, Salty water desalination using carbon nanotube sheets, Desalination 258 (2010) 182–186.
[19] H. Li, T. Lu, L. Pan, Y. Zhang, Z. Sun, Electrosorption behavior of graphene in NaCl solutions, J. Mater. Chem. 19 (2009) 6773–6779.
[20] H.B. Li, L.D. Zou, L.K. Pan, Z. Sun, Novel graphene-like electrodes for capacitive deionization, Environ. Sci. Technol. 44 (2010) 8692–8697.
[21] X. Wang, J.S. Lee, C. Tsouris, D.W. DePaoli, S. Dai, Preparation of activated mesoporous carbons for electrosorption of ions from aqueous solutions, J. Mater. Chem. 20 (2010) 4602–4608.
[22] K. Sharma, Y.H. Kim, J. Gabitto, R.T. Mayes, S. Yiacoumi, H.Z. Bilheux, L.M.H. Walker, S. Dai, C. Tsouris, Transport of ions in mesoporous carbon electrodes during capacitive deionization of high-salinity solutions, Langmuir 31 (2015) 1038–1047.
[23] D. Zhang, X. Wen, L. Shi, T. Yan, J. Zhang, Enhanced capacitive deionization of graphene/mesoporous carbon composites, Nanoscale 4 (2012) 5440–5446.
[24] Z. Peng, D. Zhang, L. Shi, T. Yan, High performance ordered mesoporous carbon/carbon nanotube composite electrodes for capacitive deionization, J. Mater. Chem. 22 (2012) 6603–6612.
[25] S. Zhao, T. Yan, H. Wang, J. Zhang, L. Shi, D. Zhang, Creating 3D hierarchical carbon architectures with micro-, meso- and macropores via a simple self-blowing strategy for flow-through deionization capacitor, ACS Appl. Mater. Interfaces 8 (2016) 18027–18035.
[26] H. Wang, T. Yan, P. Liu, G. Chen, L. Shi, J. Zhang, Q. Zhong, D. Zhang, In situ creating interconnected pores across 3D graphene architectures and their application as high performance electrodes for flow-through deionization capacitor, J. Mater. Chem. A 4 (2016) 4908–4919.
[27] Z. Wang, T. Yan, J. Fang, L. Shi, D. Zhang, Nitrogen-doped porous carbon derived from a bimetallic metal–organic framework as highly efficient electrodes for flow-through deionization capacitors, J. Mater. Chem. A 4 (2016) 10858–10868.

[28] S. Porada, L. Borchardt, M. Oschatz, M. Bryjak, J.S. Atchison, K.J. Keesman, S. Kaskel, P.M. Biesheuvel, V. Presser, Direct prediction of the desalination performance of porous carbon electrodes for capacitive deionization, Energy Environ. Sci. 6 (2013) 3700–3712.

[29] C.J. Gabelich, T.D. Tran, I.H. Suffet, Electrosorption of inorganic salts from aqueous solution using carbon aerogels, Environ. Sci. Technol. 36 (2002) 3010–3019.

[30] C.H. Hou, C.Y. Huang, A comparative study of electrosorption selectivity of ions by activated carbon electrodes in capacitive deionization, Desalination 314 (2013) 124–129.

[31] R. Zhao, M. van Soestbergen, H.H.M. Rijnaarts, A. van der Wal, M.Z. Bazant, P.M. Biesheuvel, Time-dependent ion selectivity in capacitive charging of porous electrodes, J. Colloid Interface Sci. 384 (2012) 38–44.

[32] X. Pei, J.E. Drewes, D. Heil, G. Wang, Treatment of brackish produced water using carbon aerogel-based capacitive deionization technology, Water Res. 42 (2008) 2605–2617.

[33] J.E. Dykstra, J. Dijkstra, A. van der Wal, H.V.M. Hamelers, S. Porada, On-line method to study dynamics of ion adsorption from mixtures of salts in capacitive deionization, Desalination 390 (2016) 47–52.

[34] M. Mossad, L. Zou, A study of the capacitive deionisation performance under various operational conditions, J. Hazard. Mater. 213-214 (2012) 491–497.

[35] L. Han, K.G. Karthikeyan, M.A. Anderson, K.B. Gregory, Exploring the impact of pore size distribution on the performance of carbon electrodes for capacitive deionization, J. Colloid Interface Sci. 430 (2014) 93–99.

[36] Z. Chen, H. Zhang, C. Wu, Y. Wang, W. Li, A study of electrosorption selectivity of anions by activated carbon electrodes in capacitive deionization, Desalination 369 (2015) 46–50.

[37] E.R. Nightingale, Phenomenological theory of ions salvation: effective radii of hydrated ions, J. Phys. Chem. 63 (1959) 1381–1387.

[38] H. Ohtaki, Ionic solvation in aqueous and nonaqueous solutions, Monatsh. Chem. 132 (2002) 1237–1268.

[39] Y. Li, Y. Jiang, T.J. Wang, C. Zhang, H. Wang, Performance of fluoride electrosorption using micropore-dominant activated carbon as an electrode, Sep. Purif. Technol. (2016), http://dx.doi.org/10.1016/j.seppur.2016.08.043.

[40] K. Laxman, M.T.Z. Myint, M.A. Abri, P. Sathe, S. Dobretsov, J. Dutta, Desalination and disinfection of inland brackish ground water in a capacitive deionization cell using nanoporous activated carbon cloth electrodes, Desalination 362 (2015) 126–132.